Experimental detection of quantum channel capacities

Álvaro Cuevas,[1] Massimiliano Proietti,[2,1] Mario Arnolfo Ciampini,[1] Stefano Duranti,[1,3] Paolo Mataloni,[1] Massimiliano Sacchi,[4] and Chiara Macchiavello[5]

[1]*:Quantum Optics Group, Dipartimento di Fisica, Università di Roma La Sapienza, Piazzale Aldo Moro 5, I-00185 Roma, Italy.*

[2]*:Edinburgh Mostly Quantum Lab, School of Engineering and Physical Sciences, Heriot-Watt University, David Brewster Building, EH14 4AS Edinburgh, United Kingdom*

[3]*:Dipartimento di Fisica e Geologia, Università degli Studi di Perugia, Via Pascoli snc, I-06123 Perugia, Italy.*

[4]*:Istituto di Fotonica e Nanotecnologie - Consiglio Nazionale delle Ricerche, Piazza Leonardo da Vinci 32, I-20133, Milano, Italy.*

[5]*:Dipartimento di Fisica, Università di Pavia, and INFN - Sezione di Pavia Via A. Bassi 6, I-27100 Pavia, Italy*

(Dated: December 23, 2016)

We present an efficient experimental procedure that certifies non vanishing quantum capacities for qubit noisy channels. Our method is based on the use of a fixed bipartite entangled state, where the system qubit is sent to the channel input. A particular set of local measurements is performed at the channel output and the ancilla qubit mode, obtaining lower bounds to the quantum capacities for any unknown channel with no need of a quantum process tomography. The entangled qubits have a Bell state configuration and are encoded in photon polarization. The lower bounds are found by estimating the Shannon and von Neumann entropies at the output using an optimized basis, whose statistics is obtained by measuring only the three observables $\sigma_x \otimes \sigma_x$, $\sigma_y \otimes \sigma_y$ and $\sigma_z \otimes \sigma_z$.

arXiv:1612.07754v1 [quant-ph] 22 Dec 2016

Any communication channel is unavoidably affected by noise that limits its ability to transmit information, quantified in terms of channel capacity. When the use of the channel aims to convey quantum information, its efficiency is evaluated in terms of the quantum capacity, which is the maximum number of qubits that can be reliably transmitted per channel use [1–4], and represents a central quantitative notion in quantum communications. In general the computation of the quantum capacity is a hard task since it requires a regularisation procedure over an infinite number of channel uses, and it is therefore by itself not directly accessible experimentally. Its analytical value is known mainly for some channels that have the property of degradability [5], since regularisation is not needed in this case.

In this Letter we address the issue of experimental detection of Quantum Channel Capacities. For a generic unknown channel the quantum capacity can be in principle estimated via quantum process tomography, which provides a complete reconstruction of the noise describing the action of the channel, and therefore leads to an evaluation of all its communication properties. This, however, is a demanding procedure in terms of the number of required different measurement settings, since it scales as d^4 for a finite d-dimensional quantum system [6].

Here, we are not interested in reconstructing the complete form of the noise affecting the channel, but only in detecting its quantum capacity, which is a very specific feature for which we developed a novel and less demanding procedure in terms of resources (measurements) involved. This is pursued in the same spirit as it is done, for example, in entanglement detection for composite systems [7], in parameter estimation procedures [8], and in the detection of specific properties of quantum channels, such as being entanglement-breaking [9] or non-Markovian [10].

In this Letter we report the first experiment where a lower bound to the quantum channel capacity is directly accessed by means of a number of local measurements that scales as d^2. The experiment is based on a recently proposed theoretical method [11] that can be applied to generally unknown noisy channels in arbitrary finite dimension, and has been proved to be very efficient for many examples of single qubit channels, for generalized Pauli channels in arbitrary dimension, and for two-qubit correlated Pauli and amplitude damping channels [12]. The experiment we present is based on a quantum optical implementation for various forms of noisy single-qubit channels.

We first briefly review the main theoretical ideas at the basis of the proposed implementation. The quantum capacity Q of a noisy channel $\mathcal{E}$, measured in qubits per channel use, is defined as [1–4]

$$Q = \lim_{N\to\infty} \frac{Q_N}{N} \,, \tag{1}$$

where N is the number of channel uses, $Q_N = \max_\rho I_c(\rho, \mathcal{E}_N)$, with $\mathcal{E}_N = \mathcal{E}^{\otimes N}$, and $I_c(\rho, \mathcal{E}_N)$ denotes the coherent information [13]

$$I_c(\rho, \mathcal{E}_N) = S[\mathcal{E}_N(\rho)] - S_e(\rho, \mathcal{E}_N) \,. \tag{2}$$

In the above equation $S(\rho) = -\mathrm{Tr}[\rho \log_2 \rho]$ is the von Neumann entropy and $S_e(\rho, \mathcal{E})$ represents the entropy exchange [14], i.e. $S_e(\rho, \mathcal{E}) = S[(\mathcal{I}_R \otimes \mathcal{E})(|\Psi_\rho\rangle\langle\Psi_\rho|)]$, where $|\Psi_\rho\rangle$ denotes any purification of ρ by means of an ancilla reference quantum system A, namely $\rho = \mathrm{Tr}_A[|\Psi_\rho\rangle\langle\Psi_\rho|]$.

The following chain of bounds holds

$$Q \geq Q_1 \geq I_c(\rho, \mathcal{E}_1) \geq Q_{DET} \,, \tag{3}$$

where the first two inequalities come directly from the above definitions, while the last one was proved in [11], with

$$Q_{DET} = S\left[\mathcal{E}(\rho)\right] - H(\vec{p}) \; . \tag{4}$$

In the above expression $\mathcal{E}(\rho)$ is the output state for a single use of the channel and $H(\vec{p})$ denotes the Shannon entropy for the vector of the probabilities $\{p_i\}$ corresponding to a measurement on orthogonal projectors $\{|\Phi_i\rangle\}$ in the tensor product of the ancilla and the system Hilbert spaces, namely

$$p_i = \mathrm{Tr}[(\mathcal{I}_A \otimes \mathcal{E})(|\Psi_\rho\rangle\langle\Psi_\rho|)|\Phi_i\rangle\langle\Phi_i|] \; . \tag{5}$$

The procedure to detect the lower bound Q_{DET} is the following: 1) prepare a bipartite pure state $|\Psi_\rho\rangle$; 2) send it through the channel $\mathcal{I}_A \otimes \mathcal{E}$, where the unknown channel $\mathcal{E}$ acts on one of the two subsystems; 3) measure suitable local observables on the joint output state in order to estimate $S\left[\mathcal{E}(\rho)\right]$ and $\vec{p}$, and to compute Q_{DET}. Notice that for a fixed measurement setting it is possible to infer different vectors of probabilities pertaining to different sets of orthogonal projectors. After the measurements have been performed, the detected bound Q_{DET} can then be optimized over all probability distributions that can be obtained from the used measurement settings. This last step is achieved by performing an ordinary classical processing of the measurement outcomes.

We now specify our scenario to qubit channels (dimension $d = 2$), where the new protocol only requires $d^2 - 1 = 3$ observables, in our case $\sigma_x \otimes \sigma_x$, $\sigma_y \otimes \sigma_y$, and $\sigma_z \otimes \sigma_z$ on both the ancilla and system qubit. We also consider a maximally entangled input state $|\Phi^+\rangle = 1/\sqrt{2}(|00\rangle + |11\rangle)$. The schematic representation of the procedure is shown in Fig. 1.

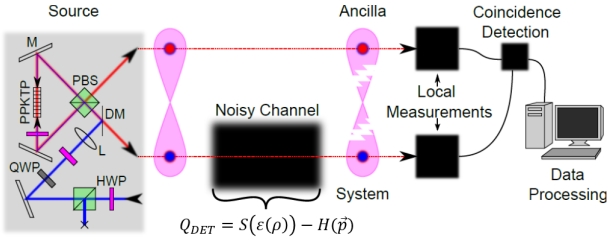

FIG. 1. **Experimental Setup.** A Sagnac interferometer source of polarization entangled photons sends the S qubit through the noisy channel, while the A qubit remains untouched. Both qubits are measured in a joint bipartite photon counter system. Here PPKTP is a periodically poled lithium niobate non-linear crystal, M is a mirror, L a converging lens, HWP a half-wave plate, QWP a quarter-wave plate, and DM a dichroic mirror.

Notice that the above observables allow to measure $\{\sigma_i\}$ on the system alone by ignoring the statistics of the measurement results on the ancilla. Since this set is a tomographically complete set on the system alone, a complete tomography of the system output state $\mathcal{E}(\rho)$ can be performed, and therefore the term $S\left[\mathcal{E}(\rho)\right]$ in Eq. (4) can be estimated exactly, as

$$S\left[\mathcal{E}(\rho)\right] = -\sum_j n_j \log_2 n_j \; , \tag{6}$$

where $\{n_j\}$ denotes the set of eigenvalues of the single-qubit output state.

Moreover, the local measurement settings $\{\sigma_x \otimes \sigma_x, \sigma_y \otimes \sigma_y, \sigma_z \otimes \sigma_z\}$ allow us to estimate the vector $\vec{p}$ pertaining to the projectors onto the following inequivalent bases [11]

$$\begin{aligned} B_1 =& \{|B_{1,1}\rangle, |B_{1,2}\rangle, |B_{1,3}\rangle, |B_{1,4}\rangle\} \\ =& \{a|\Phi^+\rangle + b|\Phi^-\rangle, -b|\Phi^+\rangle + a|\Phi^-\rangle, \\ & c|\Psi^+\rangle + d|\Psi^-\rangle, -d|\Psi^+\rangle + c|\Psi^-\rangle\}; \end{aligned} \tag{7}$$

$$\begin{aligned} B_2 =& \{|B_{2,1}\rangle, |B_{2,2}\rangle, |B_{2,3}\rangle, |B_{2,4}\rangle\}, \\ =& \{a|\Phi^+\rangle + b|\Psi^+\rangle, -b|\Phi^+\rangle + a|\Psi^+\rangle, \\ & c|\Phi^-\rangle + d|\Psi^-\rangle, -d|\Phi^-\rangle + c|\Psi^-\rangle\}; \end{aligned} \tag{8}$$

$$\begin{aligned} B_3 =& \{|B_{3,1}\rangle, |B_{3,2}\rangle, |B_{3,3}\rangle, |B_{3,4}\rangle\} \\ =& \{a|\Phi^+\rangle + ib|\Psi^-\rangle, ib|\Phi^+\rangle + a|\Psi^-\rangle, \\ & c|\Phi^-\rangle + id|\Psi^+\rangle, id|\Phi^-\rangle + c|\Psi^+\rangle\}; \end{aligned} \tag{9}$$

where $|\Phi^\pm\rangle = 1/\sqrt{2}(|00\rangle \pm |11\rangle)$ and $|\Psi^\pm\rangle = 1/\sqrt{2}(|01\rangle \pm |10\rangle)$ denote the Bell states, and a, b, c, d are real numbers, such that $a^2 + b^2 = c^2 + d^2 = 1$.

The evaluation of the Shannon entropy $H(\vec{p})$ in the B_i basis is obtained from its definition

$$H(\vec{p_i}) = -\sum_j p_{i,j} \log_2 p_{i,j} \; , \tag{10}$$

where $\vec{p_i} = \{p_{i,j}\}$ is the probability vector for the measure on the joint output state $(\mathcal{I}_A \otimes \mathcal{E})(|\Phi^+\rangle\langle\Phi^+|)$, according to Eq. (5), under the projectors $\Pi_{i,j} = |B_{i,j}\rangle\langle B_{i,j}|$. For example, in the case of B_1 we have $p_{1,j} = \langle\Pi_{1,j}\rangle$ as follows

$$\begin{aligned} p_{1,1} =& \frac{1}{4}(\langle\mathbb{I}\otimes\mathbb{I}\rangle + \langle\sigma_z\otimes\sigma_z\rangle) + \frac{ab}{2}(\langle\sigma_z\otimes\mathbb{I}\rangle + \langle\mathbb{I}\otimes\sigma_z\rangle) \\ &+ \frac{a^2-b^2}{4}(\langle\sigma_x\otimes\sigma_x\rangle - \langle\sigma_y\otimes\sigma_y\rangle) \; , \end{aligned} \tag{11}$$

$$\begin{aligned} p_{1,2} =& \frac{1}{4}(\langle\mathbb{I}\otimes\mathbb{I}\rangle + \langle\sigma_z\otimes\sigma_z\rangle) - \frac{ab}{2}(\langle\sigma_z\otimes\mathbb{I}\rangle + \langle\mathbb{I}\otimes\sigma_z\rangle) \\ &- \frac{a^2-b^2}{4}(\langle\sigma_x\otimes\sigma_x\rangle - \langle\sigma_y\otimes\sigma_y\rangle) \; , \end{aligned} \tag{12}$$

$$\begin{aligned} p_{1,3} =& \frac{1}{4}(\langle\mathbb{I}\otimes\mathbb{I}\rangle - \langle\sigma_z\otimes\sigma_z\rangle) + \frac{cd}{2}(\langle\sigma_z\otimes\mathbb{I}\rangle - \langle\mathbb{I}\otimes\sigma_z\rangle) \\ &+ \frac{c^2-d^2}{4}(\langle\sigma_x\otimes\sigma_x\rangle + \langle\sigma_y\otimes\sigma_y\rangle) \; , \end{aligned} \tag{13}$$

$$\begin{aligned} p_{1,4} =& \frac{1}{4}(\langle\mathbb{I}\otimes\mathbb{I}\rangle - \langle\sigma_z\otimes\sigma_z\rangle) - \frac{cd}{2}(\langle\sigma_z\otimes\mathbb{I}\rangle - \langle\mathbb{I}\otimes\sigma_z\rangle) \\ &- \frac{c^2-d^2}{4}(\langle\sigma_x\otimes\sigma_x\rangle + \langle\sigma_y\otimes\sigma_y\rangle) \; , \end{aligned} \tag{14}$$

where all expectation values $\langle . \rangle$ are evaluated for the joint output state $(\mathcal{I}_A \otimes \mathcal{E})(|\Phi^+\rangle\langle\Phi^+|)$. By exploiting the normalization constraints $a^2 + b^2 = c^2 + d^2 = 1$ in the above

expressions, we can see that all probabilities $p_{i,j}$, including those of the B_2 and B_3 bases, depend only on two real parameters, b and d. After collecting the measurement outcomes, the bound on Q is then maximised over the three bases B_1, B_2, B_3 and by varying b and d, namely

$$\begin{aligned} Q_{DET} &= \max_{i=1,2,3} \max_{b,d} Q_{DET}(B_i, b, d) \\ &= S[\mathcal{E}(\rho)] - \min_{i=1,2,3} \min_{b,d} H[\vec{p}(B_i, b, d)] \,. \end{aligned} \quad (15)$$

As mentioned above, this last step is performed by classical processing of the measurement outcomes, from which the set of expectation values $\{\langle \mathbb{I} \otimes \sigma_\alpha \rangle, \langle \sigma_\alpha \otimes \mathbb{I} \rangle, \langle \sigma_\alpha \otimes \sigma_\alpha \rangle, \alpha = x, y, x\}$ is obtained.

We have experimentally implemented this method by encoding the two qubits in the logical polarization basis $\{|H\rangle, |V\rangle\}$, where $|H\rangle$ ($|V\rangle$) represents the horizontal (vertical) polarization of the photons, and by considering the most common types of noisy channels in the same coding basis (see Fig. 1 for a representation of the entangled photon source). Our source of entangled photons [15] generates high purity Bell states with fidelity $F = 0.979 \pm 0.002$ and concurrence $C = 0.975$. The state is produced by two indistinguishable SPDC Type-II processes, generating photon pairs at 810 nm with a continuous wave (CW) pump at 405 nm. Photon pairs with bandwidth < 0.01 pm are detected at a frequency of more than 60.000 Hz of coincidences under a 2.5mW of pump power in a time window of 6ns. The input state is ideally the maximally entangled state $|\Phi^+\rangle$. However, due to experimental imperfections, the resulting state can be described by a Werner state $\rho_W = \frac{4F-1}{3} |\Phi^+\rangle \langle\Phi^+| + \frac{1-F}{3} I$, where F is the fidelity with respect to the ideal state and I is the 4×4 identity operator. The derivation of new detectable bounds suited for bipartite input states which are affected by isotropic noise in arbitrary finite dimension is reported in the Supplemental Material [16]. Such bounds will be used to compare our experimental results with the theoretical predictions.

In the present Letter, the procedure outlined above to obtain the lower bound to the quantum capacity of single qubit channels was tested for the following types of noise: Amplitude Damping, Phase Damping, Depolarizing and Pauli Channel. For each of them we employ $d^2 - 1$ instead of $(d^2 - 1)^2$ measurements, namely 3 versus 9 measurements for dimension of the system $d = 2$. In other words, we did not need to measure the six observables of the kind $\sigma_\alpha \otimes \sigma_\beta$ with $\alpha \neq \beta$. Our standard measurement system consists of two sets of polarization projectors, which are independently located at the reference path (ancilla-A) and at the channel output path (system-S). Each one is composed of a Quarter Wave Plate (QWP), a Half Wave Plate (HWP), and a Polarization Beam Splitter (PBS). Coincidence counts are then detected by two synchronized Avalanche Photodetectors (APDs). The expectation value for each of the Pauli operators are linear combinations of projections over the computational, diagonal, and circular basis (see [16]).

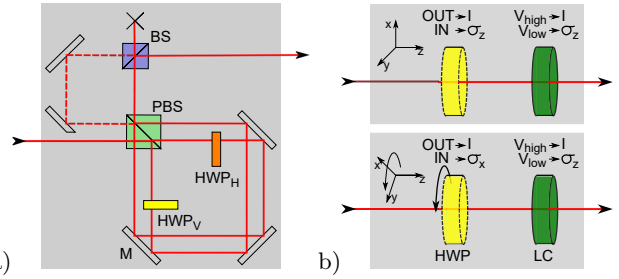

FIG. 2. **Noisy Channels. a)** Experimental scheme for a polarization Amplitude Damping channel. Given a single input qubit $|\psi\rangle = \alpha |H\rangle + \beta |V\rangle$, it uses two HWPs inside a Sagnac interferometer to apply a rotation on $|V\rangle$, while $|H\rangle$ remains unrotated, achieving K_0 and K_1. The dashed line inside the Mach-Zehnder (MZ) interferometer represents the rotated $\sqrt{\gamma}$ portion of $|V\rangle$. **b)-top** Experimental scheme for a Phase Damping channel. It applies $\mathbb{I}$ and σ_z over $|\psi\rangle$ by using an unrotated HWP and a variable voltage LC. **b)-bottom:** Experimental scheme for the Pauli and Depolarizing channels. They apply $\mathbb{I}$, σ_x, σ_y and σ_z over $|\psi\rangle$ by using a 45°-rotated HWP and the same LC.

An **Amplitude Damping Channel (ADC)** for polarization qubits with unknown probability γ can be written as $\mathcal{E}(\rho) = K_0 \rho K_0^\dagger + K_1 \rho K_1^\dagger$, where $K_0 = |H\rangle\langle H| + \sqrt{1-\gamma}|V\rangle\langle V|$, and $K_1 = \sqrt{\gamma}|H\rangle\langle V|$ translate the $|V\rangle$ polarization into $|H\rangle$ polarization, while the $|H\rangle$ remains unchanged. The experimental setup [17] consists in a Sagnac interferometer followed by a Mach-Zehnder interferometer, as shown in Fig. 2a, that allows us to perform the required noise operation. In the Sagnac loop, composed by a PBS and three mirrors, a HWP at 0 degree is put on the path of polarization $|H\rangle$, whereas a HWP at θ is put on the path of polarization $|V\rangle$. The Mach-Zehnder recombines the two outputs of the Sagnac interferometer in a non-coherent superposition, thus effectively performing the damping operation, whose amount γ depends on the angle θ [18].

A **Phase Damping Channel (PDC)** for qubits with unknown probability p can be written as $\mathcal{E}(\rho) = \left(1 - \frac{p}{2}\right) \rho + \frac{p}{2} \sigma_z \rho \sigma_z$. This map has been achieved by using a sequence of two wave retarders: a Half Wave Plate (HWP) at zero degree, which acts as σ_z, and an unrotated Liquid Crystal (LC), which acts as $\mathbb{I}$ or σ_z depending on the applied voltage on the material [19]. The system qubit is sent through the combination of this two optical elements, suffering a $\sigma_z \cdot \sigma_z = \mathbb{I}$ or $\mathbb{I} \cdot \sigma_z = \sigma_z$ operations, while the ancilla qubit remains untouched. In Fig. 2b-Top we show the schematic representation of the channel. The operation probabilities $P_z = \frac{p}{2}$ and $P_{\mathbb{I}} = 1 - P_z = 1 - \frac{p}{2}$ are derived by post-processing, by evaluating the ratio of photon coincidence counts from the measurement of the two separated experiments σ_z and $\mathbb{I}$, respectively. Then, the reconstructed channel is obtained by the mixture of two different operations, with the only constraint of the normalization condition $P_z + P_{\mathbb{I}} = 1$. The above preparation is based on the Kraus representation of a channel, where each operation can be

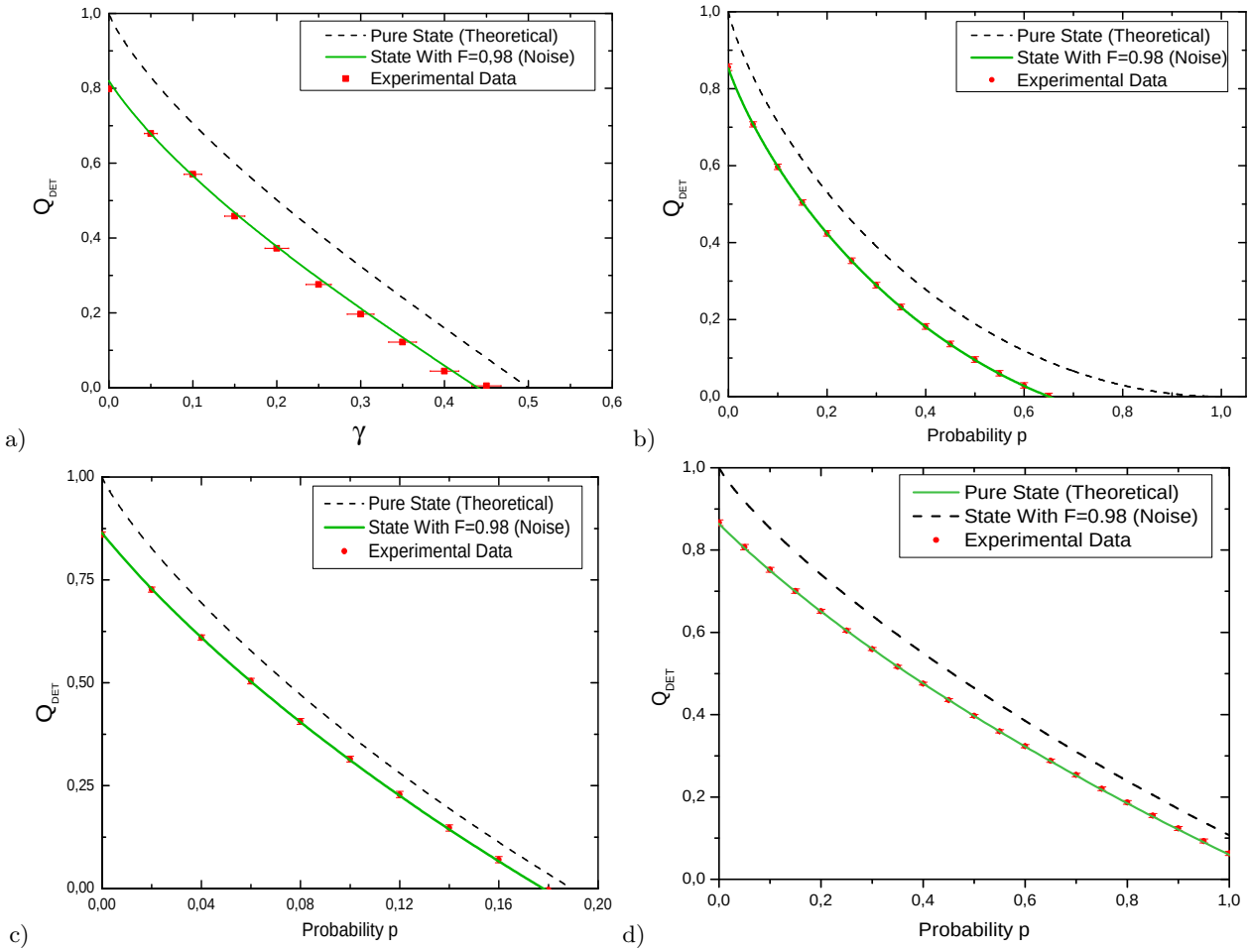

FIG. 3. **Minimal bounds Q_{DET} to the quantum channel capacity.** For the entire set of data, the red points represent the experimental values, the dashed lines corresponds to the ideal simulations for a pure maximally entangled input state, and the green lines report the theoretical predictions for an input Werner state with fidelity $F = 0.98$. **a)ADC:** The Q_{DET} depends on the damping parameter γ. Only the x-errors are present and their values were computed with the propagation of one half-degree of uncertainty in the rotation angle of HWP_V. **b)PDC:** The Q_{DET} depends on the statistical mixture of $\mathbb{I}$ and σ_z, thus on the probability vector $\vec{p} = \{P_{\mathbb{I}}, P_x, P_y, P_z\} = \{1 - \frac{p}{2}, 0, 0, \frac{p}{2}\}$. **c)DC:** The Q_{DET} depends on the balanced mixture of $\mathbb{I}$, σ_x, σ_y and σ_z, given by $\vec{p} = \{1-p, \frac{p}{3}, \frac{p}{3}, \frac{p}{3}\}$. **d)PC:** As a generalization of the channels b) and c), Q_{DET} depends on $\mathbb{I}$, σ_x, σ_y, and σ_z experiments, only restricted by the normalization condition $P_I + P_x + P_y + P_z = 1$. In our particular experiment we choose the case $\vec{p} = \{1 - \frac{p}{6}, \frac{p}{12}, \frac{p}{18}, \frac{p}{36}\}$. For b), c) and d) the errors in the y-axis were computed with the usual standard deviation from a set of a least 8 values by points, obtaining a very reduced dispersion near to the point dimensions.

achieved by an isolated experimental procedure and then linearly combined with the others to compose the entire channel action.

A **Depolarizing Channel (DC)** for qubits with unknown probability p can be written as $\mathcal{E}(\rho) = (1-p)\,\rho + \frac{p}{3}\,(\sigma_x\rho\sigma_x + \sigma_y\rho\sigma_y + \sigma_z\rho\sigma_z)$. The operations are achieved by the presence (absence) of a rotated HWP acting as σ_x when it is on the optical path or acting as $\mathbb{I}$ if taken off from the path, and by an unrotated Liquid Crystal (LC) acting as $\mathbb{I}$ or σ_z, depending on the applied voltage. Then, depending on the simultaneous actions of the HWP and the LC over ρ, the operations can be only $\mathbb{I}\cdot\mathbb{I} = \mathbb{I}$, $\sigma_z\cdot\mathbb{I} = \sigma_z$, $\sigma_z\cdot\sigma_x = i\sigma_y$ and $\mathbb{I}\cdot\sigma_x = \sigma_x$. In Fig. 2b-Bottom we show the schematic representation of the channel. Analogously to the procedure followed for the phase damping channel, the effective σ_z, σ_y, σ_x and $\mathbb{I}$ operations were applied in four separated experiments, where $P_z = P_y = P_x = \frac{p}{3}$ and $P_{\mathbb{I}} = 1 - p$ were added in post-processing of the experimental outcomes as weights of their associated operations, in order to obtain the desired mixture of measurement statistics.

The **Pauli Channel (PC)** for qubits with unknown probability p can be written as $\mathcal{E}(\rho) = P_{\mathbb{I}}\rho + P_x\sigma_x\rho\sigma_x + P_y\sigma_y\rho\sigma_y + P_z\sigma_z\rho\sigma_z$ and has been implemented using the the same procedure presented in the depolarizing channels. However, in this case there is no restriction on the choice of P_i except for the normalization condition $P_{\mathbb{I}} + P_z + P_y + P_x = 1$.

In Fig. 3 we show the experimental measurements of Q_{DET} for a prepared ADC a), PDC b), DC c) and PC

d). The dashed lines correspond to the theoretical predictions for an ideal pure maximally entangled input state, while the green lines report the theoretical predictions derived in [16] for an input Werner state with fidelity $F = 0.98$, corresponding to the state generated by our source. In all the four cases the results exhibit an excellent agreement with the theoretical predictions for our source (green lines), thus proving the effectiveness of the method and assessing efficiently the lower bound Q_{DET} to the quantum capacity of noisy channels with the most common kinds of noise. In particular, for the ADC the exact value of the capacity is known [20], and it turns out to be non-zero for $\gamma < 1/2$. In our experiment we can certify non vanishing values of the quantum capacity for the ADC for $\gamma < 0.45$ (see Fig. 3a). Also for the dephasing channel the quantum capacity is known [5], and it coincides with the dashed theoretical curve in Fig. 3b, which gives a non vanishing value for $p \neq 1$. As we can see, our experimental method allows one to certify a nonzero channel capacity for values of p up to 0.65. For the depolarising channel and, more generally, for the Pauli channel only lower bounds to the channel capacities are known [21]. In these cases we can see that with the present source the procedure is quite efficient and allows one to certify a nonzero channel capacity for values of $p \leq 0.18$, when the best theoretical lower bound predicts a nonzero channel capacity up to $p = 0.1892$.

In conclusion, we have performed an experiment to detect efficient lower bounds to the quantum capacity of qubit communication channels. Our technique does not require any prior knowledge of the quantum channel, and can be applied to any kind of unknown noise. The principal feature of the technique resides on the smaller number of measurement settings with respect to a full process tomography, and is in very good agreement with the theoretical prediction for the source we used. To the best of our knowledge this is the first experiment where the quantum capacity of a noisy channel is directly accessed. Furthermore, the detectable bounds we have provided give lower bounds to the private information and to the entanglement-assisted classical capacity, as emphasized in [11].

These results represent an important step toward an efficient experimental characterization of quantum channels such as those used in quantum cryptography, quantum teleportation, and quantum dense coding.

[1] S. Lloyd, Phys. Rev. A **55**, 1613 (1997).
[2] H. Barnum, M. A. Nielsen, and B. Schumacher, Phys. Rev. A **57**, 4153 (1998).
[3] I. Devetak, IEEE Trans. Inf. Theory **51**, 44 (2003).
[4] P. Hayden, M. Horodecki, A. Winter, and J. Yard, Open Sys. Inf. Dyn. **15**, 7 (2008).
[5] I. Devetak and P. Shor, Comm. Math. Phys. **256**, 287 (2005).
[6] I. L. Chuang and M. A. Nielsen, Journal of Modern Optics **44**, 11, 2455 (1997)
[7] O. Gühne, P. Hyllus, D. Bruß, A. Ekert, M. Lewenstein, C. Macchiavello, and A. Sanpera, Phys. Rev. A **66**, 062305 (2002).
[8] G. M. D'Ariano, M. G. A. Paris, and M. F. Sacchi, Phys. Rev. A **62**, 023815 (2000).
[9] C. Macchiavello and M. Rossi, Phys. Rev. A **88**, 042335 (2013); A. Orieux, L. Sansoni, M. Persechino, P. Mataloni, M. Rossi, and C. Macchiavello, Phys. Rev. Lett. **111**, 220501 (2013).
[10] D. Chruscinski, C. Macchiavello, and S. Maniscalco, arXiv:1607.02256.
[11] C. Macchiavello and M. F. Sacchi, Phys. Rev. Lett. **116**, 140501 (2016).
[12] C. Macchiavello and M. F. Sacchi, Phys. Rev. A **94**, 052333 (2016).
[13] B. W. Schumacher and M. A. Nielsen, Phys. Rev. A **54**, 2629 (1996).
[14] B. W. Schumacher, Phys. Rev. A **54**, 2614 (1996).
[15] A. Fedrizzi, et al., Optics Express **15.23**, 15377 (2007).
[16] See Supplemental Material
[17] A. Cuevas, A. Mari, A. De Pasquale, A. Orieux, M. Massaro, F. Sciarrino, P. Mataloni, and V. Giovannetti, arXiv:1604.08350.
[18] M. P. Almeida, F. de Melo, M. Hor-Meyll, A. Salles, S. P. Walborn, P. H. Souto Ribeiro, and L. Davidovich, Science **316**, 5824, 579 (2007).
[19] N. K. Bernardes, A. Cuevas, A. Orieux, C. H. Monken, P. Mataloni, F. Sciarrino, and M. F. Santos, Sci. Rep. **5**, 17520 (2015).
[20] V. Giovannetti and R. Fazio, Phys. Rev. A **71**, 032314 (2005).
[21] D. Di Vincenzo, P. W. Shor, and J. Smolin, Phys. Rev. A **57**, 830 (1998).

Appendix: Supplemental Material

On the effect of noise of the input state in the experimental detection of quantum channel capacities.

The theoretical results of Ref. [11], summarized in Eqs. (3–5) of the Letter, were derived under the assumption of sending a pure bipartite state at the input of the unknown channel. Realistically, as in the present experimental set-up, the generated input state will be affected by noise, thus producing a *mixed* state at the channel input.

Specifically, since our source indeed generates a maximally entangled state affected by isotropic noise, in the following, for arbitrary finite dimension d, we consider an isotropic noise map $\mathcal{N}$, leading to a bipartite mixed input state ν given by the convex combination of a maximally entangled state $|\Phi^+\rangle = \sum_{n=0}^{d-1} |n\rangle|n\rangle/\sqrt{d}$ and the totally mixed state $\frac{1}{d^2} I \otimes I$. Then, we can write

$$\nu \equiv (I \otimes \mathcal{N})|\Phi^+\rangle\langle\Phi^+| = (\mathcal{N} \otimes I)|\Phi^+\rangle\langle\Phi^+| = \frac{d^2F-1}{d^2-1}|\Phi^+\rangle\langle\Phi^+| + \frac{1-F}{d^2-1} I \otimes I \,, \tag{A.1}$$

in terms of the fidelity with the ideal maximally entangled state, namely $F = \langle\Phi^+|\nu|\Phi^+\rangle$.

As long as the noise map $\mathcal{N}$ acts on maximally entangled states, its action can be equivalently ascribed to the system or the ancilla qudit. For this reason the use of a noisy bipartite state as in Eq. (A.1) for our detection protocol is equivalent to having a perfect input $|\Phi^+\rangle$ along with a quantum measurement degraded by the isotropic dual map $\mathcal{N}^\vee$ (the map in the Heisenberg picture). In fact, for any measurement basis $\{|\Phi_i\rangle\}$ the reconstructed probabilities are

$$\begin{aligned} p_i &= \mathrm{Tr}[(\mathcal{I}_A \otimes \mathcal{E})(\mathcal{I}_A \otimes \mathcal{N})(|\Phi^+\rangle\langle\Phi^+|)|\Phi_i\rangle\langle\Phi_i|] = \mathrm{Tr}[(\mathcal{I}_A \otimes \mathcal{E})(|\Phi^+\rangle\langle\Phi^+|)(\mathcal{N}^\vee \otimes \mathcal{I})(|\Phi_i\rangle\langle\Phi_i|)] \\ &= \mathrm{Tr}[(\mathcal{I}_A \otimes \mathcal{E})(|\Phi^+\rangle\langle\Phi^+|)\Pi_i] \,, \end{aligned} \tag{A.2}$$

where

$$\Pi_i \equiv (\mathcal{N}^\vee \otimes \mathcal{I})(|\Phi_i\rangle\langle\Phi_i|) \tag{A.3}$$

is generally the element of a POVM. Then, in order to take into account the effect of noise, we need to generalize the bound of Ref. [11]

$$S_e\left(\rho, \mathcal{E}\right) \leq H(\vec{p}) \,, \tag{A.4}$$

to the case of a probability vector $\vec{p}$ pertaining to an arbitrary POVM $\{\Pi_i\}$ for the tensor product of the reference and system Hilbert spaces, where

$$p_i = \mathrm{Tr}[(\mathcal{I}_A \otimes \mathcal{E})(|\Psi_\rho\rangle\langle\Psi_\rho|)\Pi_i] \,. \tag{A.5}$$

In the following we provide such a generalization. Let us consider a density matrix σ, along with its spectral decomposition $\sigma = \sum_j s_j |\phi_j\rangle\langle\phi_j|$, and let us define the conditional probability $p(i|j) = \langle\phi_j|\Pi_i|\phi_j\rangle$. Clearly, one has $p_i \equiv \mathrm{Tr}[\sigma\Pi_i] = \sum_j s_j p(i|j)$. Then,

$$\begin{aligned} S(\sigma) - H(\vec{p}) &= \sum_i p_i \log_2 p_i - \sum_j s_j \log_2 s_j = \sum_{i,j} s_j p(i|j)(\log_2 p_i - \log_2 s_j) \\ &\leq \log_2 \left(\sum_{i,j} s_j p(i|j) \frac{p_i}{s_j} \right) = \log_2 \vec{r} \cdot \vec{p} \,, \end{aligned} \tag{A.6}$$

where we used Jensen's inequality, and defined $\vec{r}$ with vector components $r_i = \sum_j \langle\phi_j| \Pi_i |\phi_j\rangle$. Upon choosing $\sigma = (\mathcal{I}_R \otimes \mathcal{E})(|\Psi_\rho\rangle\langle\Psi_\rho|)$, one obtains the more general bound

$$S_e\left(\rho, \mathcal{E}\right) \equiv S(\sigma) \leq H(\vec{p}) + \log_2 \vec{t} \cdot \vec{p} \,, \tag{A.7}$$

with p_i as in Eq. (A.5) and $t_i \equiv \mathrm{Tr}[\Pi_i] \geq r_i$. Then, the detected quantum capacity Q_{DET} in Eq. (4) of the Letter is simply replaced with

$$Q_{DET} = S\left[\mathcal{E}(\rho)\right] - H(\vec{p}) - \log_2 \vec{t} \cdot \vec{p} \,, \tag{A.8}$$

in terms of the noisy reconstructed probabilities of Eq. (A.2).

Notice now that for any unital noise map (as the isotropic-noise one), the dual map is trace-preserving. Hence, if Π_i is of the form as in Eq. (A.3), one has $t_i \equiv \mathrm{Tr}[\Pi_i] = 1$. Then, the last term in (A.8) vanishes.

Let us see the effect of noise on the quantum capacity detection for specific channels.

1) Amplitude Damping Channel for qubits

$$\mathcal{E}(\rho) = K_0 \rho K_0^\dagger + K_1 \rho K_1^\dagger \,, \tag{A.9}$$

where $K_0 = |0\rangle\langle 0| + \sqrt{1-\gamma}|1\rangle\langle 1|$ and $K_1 = \sqrt{\gamma}|0\rangle\langle 1|$.

For an input state as in Eq. (A.1), the bipartite output is given by

$$\begin{aligned}(\mathcal{I}_A \otimes \mathcal{E})\nu = (c_1\gamma_+ + c_2)\,|\Phi^+\rangle\langle\Phi^+| + (c_1\gamma_- + c_2)\,|\Phi^-\rangle\langle\Phi^-| + \frac{\gamma}{4}(|\Phi^+\rangle\langle\Phi^-| + |\Phi^-\rangle\langle\Phi^+|) \\ + \frac{1}{4}(\gamma c_1 + 4c_2)(|\Psi^+\rangle\langle\Psi^+| + |\Psi^-\rangle\langle\Psi^-|) - \frac{\gamma}{4}(|\Psi^+\rangle\langle\Psi^-| + |\Psi^-\rangle\langle\Psi^+|)\,,\end{aligned} \tag{A.10}$$

with $\gamma_\pm = \frac{1}{4}(1 \pm \sqrt{1-\gamma})^2$, $c_1 = (4F-1)/3$, and $c_2 = (1-F)/3$. The reduced output state is given by $\mathcal{E}\left(\frac{I}{2}\right) = \frac{1}{2}(I + \gamma\sigma_z)$, hence it has von Neumann entropy $S\left[\mathcal{E}\left(\frac{I}{2}\right)\right] = H_2\left(\frac{1-\gamma}{2}\right)$. By performing the local measurement of $\sigma_x \otimes \sigma_x$, $\sigma_y \otimes \sigma_y$, and $\sigma_z \otimes \sigma_z$, estimating the von Neumann entropy $S\left[\mathcal{E}\left(\frac{I}{2}\right)\right]$, and optimising $\vec{p}$, one can detect the bound

$$Q \geq Q_{DET} = H_2\left(\frac{1-\gamma}{2}\right) - H(\vec{p})\,, \tag{A.11}$$

where the optimal vector of probabilities is given by

$$\begin{aligned}\vec{p} = \Bigg(&\frac{2 + 4F(1-\gamma) + \gamma + \sqrt{4(1-4F)^2(1-\gamma) + 9\gamma^2}}{12}, \frac{2 + 4F(1-\gamma) + \gamma - \sqrt{4(1-4F)^2(1-\gamma) + 9\gamma^2}}{12}, \\ &\frac{(1-F)(1-\gamma)}{3}, \frac{2 + \gamma - 2F(1-\gamma)}{6}\Bigg)\,.\end{aligned} \tag{A.12}$$

Such probabilities correspond to the optimal basis

$$\{a|\Phi^+\rangle + b|\Phi^-\rangle, -b|\Phi^+\rangle + a|\Phi^-\rangle, \frac{1}{\sqrt{2}}(|\Psi^+\rangle + |\Psi^-\rangle) \equiv |01\rangle, \frac{1}{\sqrt{2}}(|\Psi^+\rangle - |\Psi^-\rangle) \equiv |10\rangle\}\,, \tag{A.13}$$

where

$$a = \sqrt{\frac{\cosh\eta + 1}{2\cosh\eta}}\,, \qquad b = \sqrt{\frac{\cosh\eta - 1}{2\cosh\eta}}\,, \tag{A.14}$$

with $\eta \equiv \operatorname{arcsinh}\left(\frac{3\gamma}{2(4F-1)\sqrt{1-\gamma}}\right)$. The case of amplitude damping channel is a relevant example showing that the Bell basis can be sub-optimal for the quantum capacity certification.

2) For the Phase Damping Channel for qubits

$$\mathcal{E}(\rho) = \left(1 - \frac{p}{2}\right)\rho + \frac{p}{2}\sigma_z \rho \sigma_z\,, \tag{A.15}$$

one has

$$Q = Q_1 = 1 - H_2\left(\frac{p}{2}\right) \geq Q_{DET} = 1 - H(\vec{p})\,, \tag{A.16}$$

where the vector of probabilities $\vec{p}$ is given by

$$\vec{p} = \left\{\left(1 - \frac{p}{2}\right)F + \frac{p}{2}\frac{1-F}{3}, \frac{p}{2}F + \left(1 - \frac{p}{2}\right)\frac{1-F}{3}, \frac{1-F}{3}, \frac{1-F}{3}\right\}\,, \tag{A.17}$$

which corresponds to the Bell basis.

3) For the Depolarizing Channel in dimension d

$$\mathcal{E}(\rho) = \left(1 - p\frac{d^2}{d^2-1}\right)\rho + p\frac{d^2}{d^2-1}\frac{I}{d}\,, \tag{A.18}$$

the detectable bound is now

$$Q \geq Q_{DET} = \log_2 d - H_2(p') - p'\log_2(d^2-1)\,, \tag{A.19}$$

where

$$p' = \frac{d^2[1 - F(1-p)] + F - p - 1]}{d^2 - 1} \, . \tag{A.20}$$

For qubits

$$Q \geq Q_{DET} = 1 - H_2(p') - p' \log_2 3 \, , \tag{A.21}$$

with $p' = (1-F) + \frac{p}{3}(4F-1)$. The reconstructed probabilities for the Bell basis $\{|\Phi^+\rangle, |\Phi^-\rangle, |\Psi^+\rangle, |\Psi^-\rangle\}$ correspond to $\{1-p', \frac{p'}{3}, \frac{p'}{3}, \frac{p'}{3}\}$.

4) For a Pauli Channel in dimension d

$$\mathcal{E}(\rho) = \sum_{m,n=0}^{d-1} p_{mn} U_{mn} \rho U_{mn}^{\dagger} \, , \tag{A.22}$$

with $U_{mn} = \sum_{k=0}^{d-1} e^{\frac{2\pi i}{d} km} |k\rangle\langle (k+n) \bmod d|$, one has

$$Q \geq Q_{DET} = \log_2 d - H(\vec{p}') \, , \tag{A.23}$$

where $\vec{p}'$ is the d^2-dimensional vector of probabilities pertaining to the generalised Bell projectors, whose components are given by

$$p'_{mn} = \frac{1}{d^2 - 1}[(d^2 F - 1) p_{mn} + 1 - F] \, . \tag{A.24}$$

For the qubit case, $\mathcal{E}(\rho) = \sum_{i=0}^{3} p_i \sigma_i \rho \sigma_i$, and $p'_i = \frac{1}{3}[(4F-1)p_i + 1 - F]$.

Experimental Expectation Values

The expectation values of the measured observables on the joint ancilla-system output states are given by

$$\langle \sigma_z \otimes \sigma_z \rangle = \frac{1}{N_z} CC(|H\rangle\langle H| \otimes |H\rangle\langle H| - |H\rangle\langle H| \otimes |V\rangle\langle V| - |V\rangle\langle V| \otimes |H\rangle\langle H| + |V\rangle\langle V| \otimes |V\rangle\langle V|), \tag{A.25}$$

$$\langle \sigma_y \otimes \sigma_y \rangle = \frac{1}{N_y} CC(|R\rangle\langle R| \otimes |R\rangle\langle R| - |R\rangle\langle R| \otimes |L\rangle\langle L| - |L\rangle\langle L| \otimes |R\rangle\langle R| + |L\rangle\langle L| \otimes |L\rangle\langle L|), \tag{A.26}$$

$$\langle \sigma_x \otimes \sigma_x \rangle = \frac{1}{N_x} CC(|+\rangle\langle +| \otimes |+\rangle\langle +| - |+\rangle\langle +| \otimes |-\rangle\langle -| - |-\rangle\langle -| \otimes |+\rangle\langle +| + |-\rangle\langle -| \otimes |-\rangle\langle -|), \tag{A.27}$$

$$\langle \mathbb{I} \otimes \mathbb{I} \rangle = 1, \tag{A.28}$$

$$\langle \sigma_z \otimes \mathbb{I} \rangle = \frac{1}{N_z} CC(|H\rangle\langle H| \otimes |H\rangle\langle H| + |H\rangle\langle H| \otimes |V\rangle\langle V| - |V\rangle\langle V| \otimes |H\rangle\langle H| - |V\rangle\langle V| \otimes |V\rangle\langle V|), \tag{A.29}$$

$$\langle \sigma_y \otimes \mathbb{I} \rangle = \frac{1}{N_y} CC(|R\rangle\langle R| \otimes |R\rangle\langle R| + |R\rangle\langle R| \otimes |L\rangle\langle L| - |L\rangle\langle L| \otimes |R\rangle\langle R| - |L\rangle\langle L| \otimes |L\rangle\langle L|), \tag{A.30}$$

$$\langle \sigma_x \otimes \mathbb{I} \rangle = \frac{1}{N_x} CC(|+\rangle\langle +| \otimes |+\rangle\langle +| + |+\rangle\langle +| \otimes |-\rangle\langle -| - |-\rangle\langle -| \otimes |+\rangle\langle +| - |-\rangle\langle -| \otimes |-\rangle\langle -|), \tag{A.31}$$

$$\langle \mathbb{I} \otimes \sigma_z \rangle = \frac{1}{N_z} CC(|H\rangle\langle H| \otimes |H\rangle\langle H| - |H\rangle\langle H| \otimes |V\rangle\langle V| + |V\rangle\langle V| \otimes |H\rangle\langle H| - |V\rangle\langle V| \otimes |V\rangle\langle V|), \tag{A.32}$$

$$\langle \mathbb{I} \otimes \sigma_y \rangle = \frac{1}{N_y} CC(|R\rangle\langle R| \otimes |R\rangle\langle R| - |R\rangle\langle R| \otimes |L\rangle\langle L| + |L\rangle\langle L| \otimes |R\rangle\langle R| - |L\rangle\langle L| \otimes |L\rangle\langle L|), \tag{A.33}$$

$$\langle \mathbb{I} \otimes \sigma_x \rangle = \frac{1}{N_x} CC(|+\rangle\langle +| \otimes |+\rangle\langle +| - |+\rangle\langle +| \otimes |-\rangle\langle -| + |-\rangle\langle -| \otimes |+\rangle\langle +| - |-\rangle\langle -| \otimes |-\rangle\langle -|), \tag{A.34}$$

with

$$N_z = CC(|H\rangle\langle H| \otimes |H\rangle\langle H| + |H\rangle\langle H| \otimes |V\rangle\langle V| + |V\rangle\langle V| \otimes |H\rangle\langle H| + |V\rangle\langle V| \otimes |V\rangle\langle V|), \tag{A.35}$$

$$N_y = CC(|R\rangle\langle R| \otimes |R\rangle\langle R| + |R\rangle\langle R| \otimes |L\rangle\langle L| + |L\rangle\langle L| \otimes |R\rangle\langle R| + |L\rangle\langle L| \otimes |L\rangle\langle L|), \tag{A.36}$$

$$N_x = CC(|+\rangle\langle +| \otimes |+\rangle\langle +| + |+\rangle\langle +| \otimes |-\rangle\langle -| + |-\rangle\langle -| \otimes |+\rangle\langle +| + |-\rangle\langle -| \otimes |-\rangle\langle -|). \tag{A.37}$$

In the above equations $CC(|i\rangle\langle i| \otimes |j\rangle\langle j|)$ denotes the coincident photon detections of the state within a time window, associated to the projection on the state $|i\rangle \otimes |j\rangle$ of the ancilla and system qubits, with $i, j = H, V, L, R, +, -$. The

different bases are characterized as logical $\{|H\rangle, |V\rangle\}$, circular $\{|L\rangle = \frac{1}{\sqrt{2}}(|H\rangle + i\,|V\rangle), |R\rangle = \frac{1}{\sqrt{2}}(|H\rangle - i\,|V\rangle)\}$, or diagonal $\{|+\rangle = \frac{1}{\sqrt{2}}(|H\rangle + |V\rangle), |-\rangle = \frac{1}{\sqrt{2}}(|H\rangle - |V\rangle)\}$, while N_z, N_y, and N_x are the normalization factors also expressed in terms of coincidences.

Equations (A.29-A.31) are equivalent to take a partial trace of the S-qubit, and measure exclusively the A-qubit by the triggering the coincidences with the detection of S. Similarly, equations (A.32-A.34) are equivalent to take a partial trace of the A-qubit, and measure exclusively the S-qubit by the triggering the coincidences with the detection of A.